

# Var-CNN and DynaFlow: Improved Attacks and Defenses for Website Fingerprinting

Sanjit Bhat

*MIT PRIMES*

*sanjit.bhat@gmail.com*

David Lu

*MIT PRIMES*

*davidboxboro@gmail.com*

Albert Kwon

*MIT*

*kwonal@mit.edu*

Srinivas Devadas

*MIT*

*devadas@mit.edu*

## Abstract

In recent years, there have been many works that use website fingerprinting techniques to enable a local adversary to determine which website a Tor user is visiting. However, most of these works rely on manually extracted features, and thus are fragile: a small change in the protocol or a simple defense often renders these attacks useless. In this work, we leverage deep learning techniques to create a more robust attack that does not require any manually extracted features. Specifically, we propose Var-CNN, an attack that uses model variations on convolutional neural networks with both the packet sequence and packet timing data. In open-world settings, Var-CNN attains higher true positive rate and lower false positive rate than any prior work at 90.9% and 0.3%, respectively. Moreover, these improvements are observed even with low amounts of training data, where deep learning techniques often suffer.

Given the severity of our attacks, we also introduce a new countermeasure, DynaFlow, based on dynamically adjusting flows to protect against website fingerprinting attacks. DynaFlow provides a similar level of security as current state-of-the-art and defeats all attacks, including our own, while being over 40% more efficient than existing defenses. Moreover, unlike many prior defenses, DynaFlow can protect dynamically generated websites as well.

## 1 Introduction

Due to increases in mass surveillance and other attacks on privacy, many Internet users have turned to Tor [12] to protect their anonymity. Over the years, Tor has grown to over 6,000 volunteer servers and 4 million daily users [1]. Tor protects the users’ identities by routing each packet through a number of Tor servers. Each server learns only the immediate hop before and after itself, and as a result, no single server learns both the identity of the user and the destination of the packet.

Unfortunately, Tor does not provide anonymity against a powerful global adversary that can monitor a significant portion of the traffic on the Tor network due to traffic analysis attacks. In such attacks, the adversary monitors the traffic entering and leaving the Tor network.

Then, she recognizes patterns in the network traffic, such as packet size and timing, to correlate traffic across the ends of the network and determine the identities of two communicating parties. Recently, a new variant of traffic analysis attack called *website fingerprinting* (WF) attack allows an adversary who observes only the connection between the user and the Tor network to identify the website the user is visiting. Here, an adversary first identifies traffic patterns exhibited by certain websites, and the adversary extracts *features* of the traffic pattern to create a digital fingerprint for each website. Finally, the adversary compares these fingerprints with a user’s network traffic and determines which website a user is visiting.

Most prior website fingerprinting attacks [9, 39, 16, 26, 15, 5, 27, 40, 31, 14, 41, 32, 8] have used *manually* extracted features to carry out the attack. That is, the authors studied different protocols carefully (such as HTTP, Tor, etc.), and manually determined features like the total number of packets and transmission time that could potentially be used to identify the website from the network trace. While these attacks have yielded high accuracy in their original settings, they unfortunately fail to deliver against defenses that modify those particular features. For instance, an attack that primarily relied on the cumulative length of the packets [31] performs significantly worse against a defense that simply perturbs the length.

In this work, we introduce Var-CNN, a novel website fingerprinting attack based on deep learning – in particular, variations of convolutional neural networks (CNN) – and DynaFlow, a new defense with strong security properties. Recently, deep learning has become the state-of-art machine learning technique in many different domains. One of the main advantages of deep learning is that the algorithm extracts the features automatically. As a result, it can often catch abstract and higher level features not easily available to humans, and the attack need not rely on a set of features specific to a particular protocol or a system. As a result, the attacker can quickly adapt to changes in protocols or new defenses.

Var-CNN uses two optimized CNNs to automatically extract features from both the packet sequence and the packet timing to identify the traffic pattern. We then

combine the results of these two CNNs to yield a final, more powerful classifier. We show that Var-CNN using automated feature extraction can outperform all prior work with manually extracted features: Against the data set introduced by Wang et al. [40], Var-CNN achieves 90.9% true positive rate and 0.3% false positive rate, and outperforms prior-art [14] which achieved 88% true positive rate and 0.5% false positive rate, despite the relatively small training set by deep learning standards.

In addition to the attack, we also present a new defense, DynaFlow. This defense ensures that there is always a flow of packets by introducing dummy packets and delays between packets, similar to prior defenses [13, 7]. Unlike those works, DynaFlow allows for *dynamic* tuning of the parameters to adjust the flow, and thus reduces the overhead of the defense without sacrificing security. For example, to limit the attacker’s accuracy to 50%, DynaFlow results in overhead (combined bandwidth and latency) of about 90%, while Tamaraw [7] requires 130% overhead. Furthermore, many prior defenses [40, 29, 42] require a database with network traces of websites, and could not protect dynamically generated websites that vary significantly from websites in the database. DynaFlow, on the other hand, does not require such a database, and can protect even dynamic contents.

In summary, the contributions of this paper are the following:

- We propose a new website fingerprinting attack using convolutional neural networks that extracts features automatically from both the packet sequences and packet timing information.
- We evaluate our attack on the data set from Wang et al. [40], and compare against prior-art [40, 14, 4]. We achieve 93.2% accuracy in the closed-world setting (2% higher than prior-art), and achieve 90.9% true positive rate (2.9% higher) and 0.3% false positive rate (0.2% lower) in the open-world setting.
- We propose a new defense, DynaFlow, that improves on several aspects of prior defenses [13, 7] and integrates new techniques to achieve the same level of security with lower overhead. Our evaluation shows that for similar levels of security, DynaFlow requires significantly less overhead (often 40% lower overhead) compared to Tamaraw [7].

We show that website fingerprinting with automatic feature extraction can outperform state-of-the-art hand-tuned algorithms, and that strong defenses need not incur a large overhead.

## 2 Background and related work

In this section, we present prior work on website fingerprinting attacks and defenses.

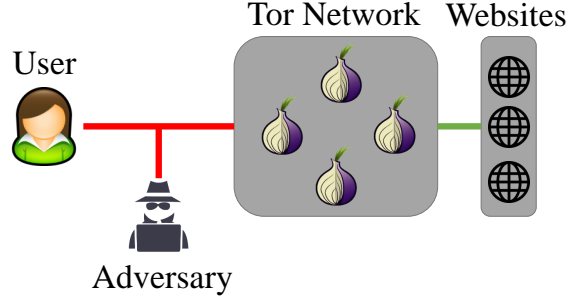


Figure 1: The Website Fingerprinting threat model.

### 2.1 Website fingerprinting attacks

Tor [12] consists of decentralized volunteer servers that relays the users’ packets without any delays or cover traffic. While this has allowed Tor to scale to a large number of users, this also enables adversaries monitoring traffic entering and leaving the Tor network to potentially deanonymize users. In particular, website fingerprinting (WF) attacks allow an adversary that monitors just the connection between a user and the network to identify which website the user is visiting. To do so, the adversary first creates a large database of traffic patterns exhibited by certain websites she wants to identify, and attempts to classify the traffic pattern of the user using the database.

#### 2.1.1 Threat model and assumptions

In this work, we assume the same adversary model as prior work [32, 13, 8, 41, 40, 31, 14]. The adversary is a passive observer (meaning she will not drop, modify, or insert any packets), who monitors the connection between a user and the Tor network, as shown in Figure 1. There are many realistic adversaries that map to this model: e.g., routers, internet service providers, autonomous services, compromised Tor servers, etc. The adversary is interested in identifying visitors of a number of websites, which we call *monitored* websites; similarly, we call all others *unmonitored* websites. The adversary is assumed to visit the websites on her own and collect *traces*, the sequence of packets and their time stamps generated while visiting a website, to create a database of traces. Once the database is created, she monitors and collects users’ traces, and attempts to identify which website corresponds to which trace. We also assume that the user loads one website at a time and that the adversary can determine the start of a website load.

There are two different settings we consider against such an attacker, closed-world and open-world.

**Closed-world** In this setting, we assume that users only visit monitored websites. Here, we use *accuracy* to define the effectiveness of the attacker, which is sim-

ply the proportion of user traces that were identified correctly. Although the closed-world is not realistic, it is a useful measure of a classifier’s ability to distinguish between websites.

**Open-world** In the real world, users can visit websites that the adversary does not know. Open-world settings emulate this scenario, by allowing the users to visit both monitored and unmonitored websites. The adversary must first classify each trace as either an unmonitored or monitored website, and if it is a monitored website, then also identify the specific website. The effectiveness in this setting is measured by three values: *true positive rate* (TPR), the proportion of monitored websites that are classified correctly, *false positive rate* (FPR), the proportion of unmonitored websites that are incorrectly classified as a monitored website, and *precision*, the proportion of monitored websites that are correctly classified out of the total number of monitored classifications.

We now categorize prior website fingerprinting attacks into two sub-categories, manual and automated feature extraction, and describe them.

### 2.1.2 Manual feature extraction

In the past, several WF attacks have been proposed, each directing specific attention towards the susceptible components of the protocol studied. For example, early work used weaknesses in HTTP 1.0 to take advantage of distinct resource length leakage, such as the size of images, scripts, and videos [9, 39, 16]. However, subsequent protocols blocked this leakage, resulting in attacks re-focusing on unique packet lengths leaked by HTTP 1.1, VPNs, and SSH tunneling [26, 15, 5, 27]. Finally, after this information was hidden by anonymous networks such as Tor, attacks have since focused on using packet ordering information to perform fingerprinting [32, 13, 8, 41]. For example, Wang et al. used the  $k$ -NN classifier and a wide assortment of features to perform fingerprinting [40]. Panchenko et al. developed CUMUL, using an SVM and mainly relying on cumulative packet length features [31]. Finally,  $k$ -FP, the current state-of-the-art, combines Random Forests as a feature extractor for  $k$ -NN. Using a wide set of pre-extracted features, this attack achieves an 88% true positive rate (TPR) and 0.5% false positive rate (FPR) in the open-world setting [14].

Since these attacks were all designed with a specific anonymous network or protocols in mind, changes in protocol or new defenses often require a redesign of the attack. For example, Hayes et al. [14] pointed out that since CUMUL primarily relies on cumulative packet

length, it suffers significant decreases in accuracy against defenses which perturb this information.

### 2.1.3 Automated feature extraction

Recently, a few WF attacks using deep learning have been proposed. Compared to traditional attacks, these attacks perform automated feature extraction over raw input sequences, removing the need for feature re-design. Initially, Abe and Goto [4] used a Stacked-Denoising Autoencoder to achieve an 86% TPR and 2% FPR in the open-world. Next, both Rimmer et al. [34] and Sirinam et al. [37] used Convolutional Neural Networks (CNN) to achieve promising results on their own data sets. In particular, Sirinam et al. achieved over 90% TPR and less than 1% FPR by tuning the CNN parameters. Unfortunately, since neither of their data sets or codes are currently available, it is difficult to compare these works directly to prior work or our work. Moreover, all three prior works only used the packet sequence with the directional data of each packet, ignoring any timing information.

In this work, we apply non-standard techniques from deep learning to significantly improve upon results using vanilla CNNs, and evaluate our model against a well-studied data set [40] to ensure a fair comparison. In addition, we also take advantage of the inter-packet timing information to further improve TPR and FPR. Our findings indicate that automated feature extraction attacks not only perform well while remaining protocol-independent, but also outperform prior state-of-the-art attacks with manually extracted features. Our work also suggests that we potentially do not need a larger data set than traditional machine learning algorithms to train a successful deep learning model, as the data set we use [40] was initially prepared for the  $k$ -nearest neighbor algorithm.

## 2.2 Website fingerprinting defenses

To defend users from WF attacks, many prior works have proposed WF countermeasures [40, 32, 13, 6, 7, 29, 42, 21, 10, 43, 33, 28, 8]. Earlier WF defenses, known as *limited defenses*, were designed to counter existing attacks. For example, LLaMA [10, 28, 33] modifies HTTP requests by adding extra delays between requests, decoy pages [32] loads another page in parallel with the desired website to obscure the original trace, and WTF-PAD [21] hides unlikely time gaps between packets and bursts by adaptively introducing dummy packets to pad the traffic.

Over time, defenses that defeated older attacks failed against newer ones [28, 32, 33, 43, 8, 14]. Thus, recent research has focused on creating defenses with formal security guarantees that protect users against much larger classes of attackers, and provide bounds on attacker ac-

Table 1: Comparison of DynaFlow with prior defenses.

	Low Latency	Low Bandwidth Usage	Strong Security Guarantees	Protects Dynamic Content	No Database Required	Highly Tunable
DynaFlow	✓	✓	✓	✓	✓	✓
BuFLO [13]	✗	✗	✗	✓	✓	✗
Tamaraw [7]	✗	✗	✓	✓	✓	✗
Supersequence [40]	✗	✗	✓	✗	✗	✗
Walkie-Talkie [42]	✓	✓	✓	✗	✗	✓
Glove [29]	✗	✗	✓	✗	✗	✗
WTF-PAD [21]	✓	✓	✗	✓	✓	✗
Decoy Pages [32]	✓	✗	✗	✓	✓	✗
LLaMA [10]	✓	✓	✗	✗	✗	✗

curacy. There are two high-level classes of defenses: *supersequence* defenses and *constant-flow* defenses.

### 2.2.1 Supersequence defenses

Defenses in this class first collect a database of traffic traces of many different websites, and group the traces into sets. In each set, a “supersequence” is computed such that every trace in the set is a subsequence of the supersequence [40, 29, 42]. Then, padding is added to each trace so that every trace in the set is morphed into the supersequence, and the adversary learns that a particular trace is in a set. Walkie-Talkie [42] uses half-duplex communication and breaks each trace down into sequence of small bursts, making supersequences easier to create.

Unfortunately, supersequence defenses are difficult to deploy in practice because they require a database of web traces that must constantly be updated as websites change; in some cases, a website might change enough that its trace can no longer be fitted into the precomputed supersequence. Consequently, these defenses only apply to static websites: they do not protect websites using AJAX or JavaScript [42, 29]. Furthermore, they usually incur large overheads, often doubling the latency or bandwidth usage [29].

### 2.2.2 Constant-flow defenses

Defenses in this second class flood the network with a continuous stream of packets to prevent the adversary from identifying any meaningful patterns in the traffic, thus the name “constant-flow”. BuFLO [13], one of the first constant-flow defenses, maintained a continuous stream of packets during a page load, but still leaked the length of each trace resulting in some privacy leakage.

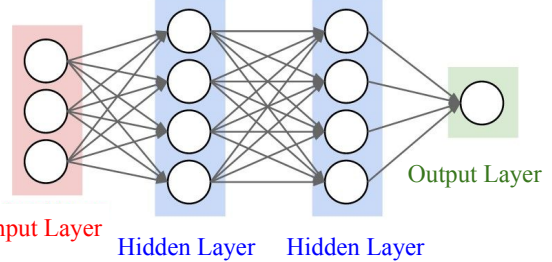


Figure 2: A deep learning neural network [22].

Tamaraw [7] increased BuFLO’s security by restricting possible trace lengths. While its security guarantees are strong, Tamaraw incurs overheads of at least 100%, even for its lightest configurations. This often causes load times to more than double.

Constant-flow defenses are easier to deploy in the real world, in part because they do not require any pre-built databases. However, these defenses usually incur high latency and bandwidth usage. Our goal is therefore to construct a defense with similar guarantees as Tamaraw but with significantly lowered overheads. Table 1 compares our defense with the top WF defenses.

## 3 Var-CNN: Model variations on CNN

We first give a short background on convolutional neural networks, and then present details of Var-CNN.

### 3.1 Convolutional neural network

Convolutional neural networks are part of a class of machine learning techniques called deep learning (Figure 2). Unlike traditional machine learning, deep learning has the expressive power to automatically extract fea-

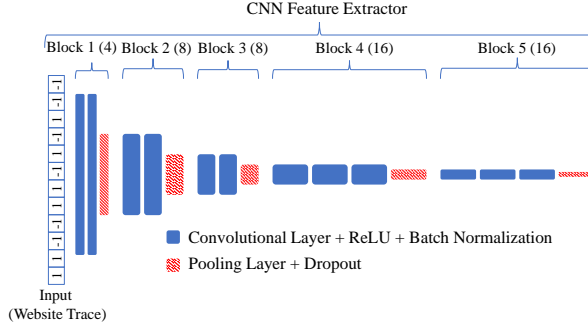


Figure 3: A graphical model of our CNN architecture. Note that rectangle sizes represent the dimensionality of data going through the layers, and numbers in parentheses next to the blocks signify the number of filters used in the convolutional layers.

tures from raw input data by using many layers and non-linear activation functions such as ReLU [25]. We use a convolutional neural network (CNN) due to its hierarchical abstraction of features. CNNs, which consist of three kinds of layers, can express complex relationships between locally-defined features to construct more abstract features [24]. Specifically, *convolutional layers* use filters to create feature maps from the input, *pooling layers* combine adjacent features from the feature maps, and *fully-connected layers* at the end of the network perform classification.

### 3.2 Details of Var-CNN

Our baseline CNN architecture (Figure 3) is based on the VGG16 network [36] used in the ImageNet competition [35]. Like VGG16, our model has five blocks, each consisting of multiple convolutional layers and a final pooling layer. Stacking multiple blocks with an increasing number of filters per block aids in higher-level feature extraction and increased expressive power, as shown by the widening graphical model. Due to computational restraints, we reduce the number of filters per block and the number of neurons in each fully-connected layer. In our tests, we noticed that these changes had little to no impact on the result.

In addition to the regular VGG16 network, we employ batch normalization to the activations of each layer to increase the speed of training [18]. In addition, we apply dropout regularization [38] at various rates to the end of each convolutional block and each fully-connected layer. Dropout ensures that a different fraction of each layer’s neurons are not used during each forward pass of the network. This helps reduce overfitting by removing reliance on individual neurons. We use variants of this CNN to train on both packet sequences and inter-packet timing, and combine the result to create a stronger classifier.

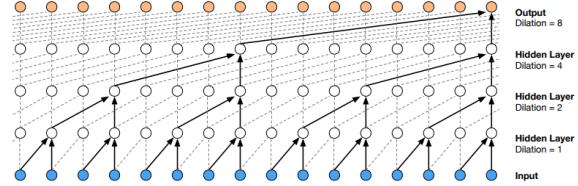


Figure 4: A pictorial representation of dilated convolutions [30].

#### 3.2.1 Dilated convolutions on packet directions

With traditional convolutional operations, filters in each layer are convolved with the input sequence to produce feature maps. However, given that filters in standard VGG16 networks span only 3 inputs at once, the network can only contextualize related packets within this small range. While this is natural in areas such as computer vision, where image pixels typically only relate to those directly around them, packet sequences inherently have a long-term temporal structure to them, as each packet depends on the previous packets sent.

Traditionally, recurrent neural networks (RNN) are used for such temporal orderings. However, the length of our packet sequence proved too long even for state-of-the-art RNN.<sup>1</sup> Instead, we build temporal understanding into our CNN model by utilizing *dilated convolutions* [44] – convolutions which skip inputs at a certain dilation rate. Intuitively, instead of taking a fine-grain view of a small input region, dilated convolutions allow the network to take a coarse, wide view of the network as shown in Figure 4. While a wide view could theoretically be achieved by increasing filter size, dilated convolutions sacrifice fine-grain detail to circumvent the drawback of decreasing computational efficiency [30].

Our model doubles dilation rates in every layer up to a certain limit, repeating the cycle after hitting the limit (i.e., dilation rates are  $\{1, 2, 4, 8, 1, 2, 4, 8, \dots\}$ ); this has been shown to be effective [44, 30], as each node in the network can cover a large number of inputs after just a few layers. Going from a dilation rate of 1, effectively a standard convolutional operation, to a dilation rate of 8, means every block of 4 layers will consider 16 inputs.

#### 3.2.2 Packet timestamps

Here, we apply a CNN on the raw, low-level timestamps of packets in addition to the inter-packet time difference between a given packet and its left and right adjacent packets. The CNN is nearly the same as the one applied

<sup>1</sup> We believe that the packet sequence is prohibitively long to train on RNNs because of vanishing gradients, wherein the gradient updates are essentially lost after backpropagating through such a long sequence.

to direction; the sole change we made was refraining to use dilated convolutions here as it burdens accuracy. Intuitively, this is because inter-packet timing is largely a local function (e.g., an outgoing packet should depend mostly on the immediate incoming packet).

Bissias et al. [5] used inter-packet timings in an early WF attack. However, compared to similar work using different features, this attack did not perform as well. More recently Wang et al. [40] used total transmission time as one of their features, and Hayes et al. [14] did a feature study using features such as inter-arrival times. As shown by Hayes et al., however, these low-level time features remained in the 40th-70th feature importance rank, essentially making them useless for classification. As we will see in §4.2.1, this model by itself does not perform as well as the direction CNN, which is consistent with conclusions of prior work. However, we describe a way to combine the two models to improve the final classifier in §3.2.4.

### 3.2.3 Basic cumulative features

In addition to automatically extracting features from the raw data, we also provide 7 basic cumulative features to the model. These features include the total number of packets, the total number of incoming packets, the total number of outgoing packets, the ratio of incoming to total packets, the ratio of outgoing to total packets, the total transmission time, and the average rate at which packets were sent. These basic features are incorporated to our attack by concatenating the output of the CNN after one fully-connected layer. After concatenation, the combined output is sent through another fully-connected layer before going to the final softmax output.

### 3.2.4 Ensemble of timing and direction

The final version of our attack, which we call *ensemble*, combines all of our models together to create a joint model stronger than any constituent. In our work, we join the direction CNN and time CNN, along with basic features, through an averaging of the final softmax output probability distributions of both models, post-training, as shown in Figure 5. By averaging the final outputs post-training rather than during training, we reduce the likelihood of overfitting, in addition to letting each model best learn how to use its feature set independent of the other model. Note that even though the timing CNN is worse than the direction CNN, post-training averaging enables the errors of both models to mitigate each other, resulting in an overall higher TPR and lower FPR than the best constituent model. We describe this phenomenon in §4.2.1 in more detail.

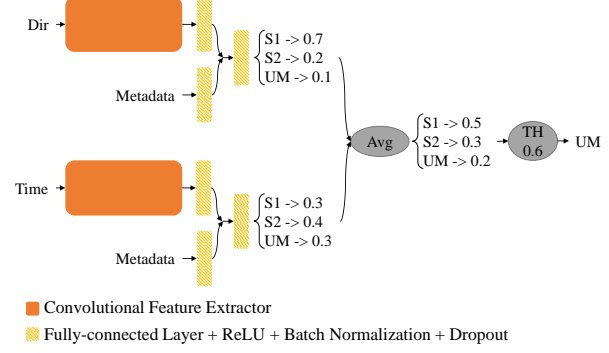


Figure 5: A graphical representation of our ensemble model. UM represents the unmonitored class, while TH signifies a minimum confidence threshold of a certain value. The internals of the convolutional feature extractor are shown in Figure 3.

### 3.2.5 Confidence threshold

As the final step of our attack, we apply a post-training threshold on the probability output of the network. If the output probability is less than this threshold, we change the predicted class to the unmonitored class (indicated by the “TH” block in Figure 5). Intuitively, this can be explained as defining a certain minimum bound on model certainty before classifying a sample. If a model is not certain about its classification of a website, we assume that the testing input only partially matches a monitored site, so we classify it as unmonitored.

The threshold constraint also allows for direct control over TPR and FPR trade-off. Prior work used methods such as classify-verify [20], using an additional classifier on top of features outputted from a primary classifier [14], and changing the number of nearest neighbors in  $k$ -NN [40, 14]. In the case of using a different model to perform final classification, this results in increased computational time due to training multiple models, and decreased accuracy due to information loss between feature extractor and classifier. Additional schemes such as classify-verify and adjusting the nearest neighbors require re-training of the model.

In Var-CNN, we can easily try different thresholds. With a threshold of 0, this is the equivalent to not applying any model constraint. When threshold is 1, we restrict the network to only output websites as monitored if it is 100% certain.

## 4 Var-CNN evaluation

In this section, we describe our experimental setup and evaluate Var-CNN.

## 4.1 Experimental setup

**Data set** We evaluate our attack on Wang et al.’s  $k$ -NN data set [40], which has been well studied by many prior works [40, 14, 31, 4]. This data set consists of 100 monitored pages (90 traces each) and 9000 unmonitored pages (1 trace each). The monitored pages were compiled from a list of blocked pages from China, UK, and Saudi Arabia, and include adult content sites, torrent trackers, social media sites, and sites with sensitive content. In contrast, the unmonitored pages are the 9,000 most popular sites compiled from Alexa [2].

Each trace contains the direction and time stamp of each packet. The numbers 1 and  $-1$  respectively denote outgoing packets (which travel toward the web server) and incoming packets (which travel toward the client). Since CNNs only take in a fixed-length input, we truncate and pad each direction and time trace to 4,096 values, a power of 2 which enables further dimensionality reduction by the pooling layers. While larger sequences increase the computational overhead, smaller sequences cause more information loss. Using a 4,096 long sequence results in 2,740 sequences which require truncating, and 15,260 which require padding.

**Train/Test Split** In our experiments, we use less than or equal to the amount of training data used by prior work. For closed-world, we use 60 instances of each monitored site for training and the remaining 30 instances for testing, the exact same as Wang et al. [40] and Hayes et al. [14], but less than the 72/18 train/test split used by Abe et al. [4].

For open-world, we use an additional 3,500 unmonitored sites for training and test on the remaining 5500 unmonitored sites. This is the same as Hayes et al. [14], slightly less than the 5000/4000 split used by Wang et al. [40], and significantly less than the 7200/1800 split used by Abe et al. [4]. To obtain an accurate estimate of the strength of our model, we run closed- and open-world test ten times, re-randomizing training and testing sets each time and reporting the average and the standard deviation.

**Model Implementation** To implement Var-CNN, we use Keras [11] with the TensorFlow [3] back end. Given that neural networks are several times quicker to run on GPUs, we run our experiments on one NVIDIA GTX 1060 with 6 GB of GPU memory.

**Parameter Searching** To determine parameters for Var-CNN, we adopt a methodology of keeping all other parameters constant while sweeping a certain range of values for one parameter. After finding an optimal value, we fix it, and then test other parameters. For further

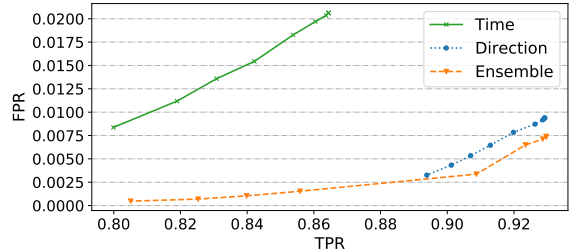


Figure 6: The TPR-FPR trade-off for direction, time, and ensemble variants of Var-CNN, as the minimum confidence threshold varies from 0 to 0.9 in 0.1 increments.

details on what specific parameters we used and for intuitions on well-performing parameter ranges, see Appendix A. Note that our parameter search was by no means extensive, especially for the Var-CNN timing model. It is entirely possible that different Var-CNN configurations perform differently on direction data versus time data, but we made a simplifying assumption to use the same configuration.

## 4.2 Experimental results

In this section, we discuss our various experiments and their implications.

### 4.2.1 Comparison of variants of Var-CNN

We first compare the three different models of CNN: direction, time, and ensemble.

Figure 6 shows a graph of TPR and FPR as we change the confidence threshold from 0.0 to 0.9. We can see that Var-CNN with direction information achieves comparable FPR to that with inter-packet timing information at 0.8%, while having 13% higher TPR at 93%. Although Var-CNN was not specifically optimized for timing, these preliminary results indicate that direction information leaks more about the trace than time (as suggested by prior work as well [14]).

While our model with direction is better than that with time, both can be effectively combined to create an overall stronger ensemble model. We see that the Var-CNN ensemble can achieve lower FPR for all comparable TPR values when compared to Var-CNN direction. For example, at a threshold of 0, Var-CNN direction and ensemble both achieve 93% TPR, but the FPR of Var-CNN ensemble is nearly 0.2% lower. Overall, this shows that even though timing information perhaps cannot be effectively used by itself, combining timing and direction allows the ensemble to take advantage of best of both models.

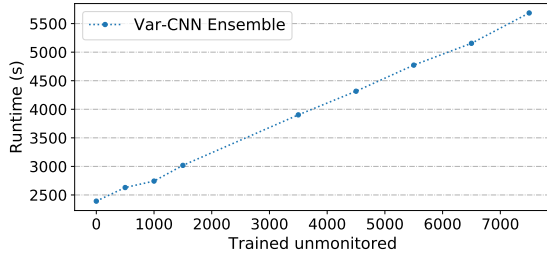


Figure 7: The total training time of Var-CNN ensemble as the number of trained unmonitored sites in the open-world increases.

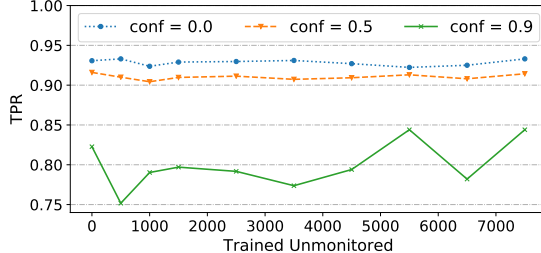


Figure 8: The Var-CNN Ensemble TPR as a function of the number of trained unmonitored sites for three different confidence settings.

#### 4.2.2 TPR-FPR trade-off

As discussed in §3.2.5, Var-CNN allows TPR-FPR trade-off by changing the confidence threshold after training is done. By using a smaller confidence constraint on this prediction, the attacker can lower FPR by assuming that unmonitored sites have a low classification accuracy. As shown by Figure 6, this assumption holds true as the FPR of an attacker goes down as the confidence interval increases. For instance, with a threshold of 0, Var-CNN ensemble achieves 0.74% FPR, while this steadily goes down to 0.07% for a threshold of 0.8. This, however, comes at the cost of TPR, as monitored websites are conservatively classified as unmonitored websites.

#### 4.2.3 Closed- and open-world results

Compared to SDAE [4], the only attack with automatic feature extraction that evaluated on the same data set, our Var-CNN ensemble outperforms it in both closed- and open-world settings. In closed-world settings, we achieve a 93.2% accuracy, 5.2% higher than SDAE. In open-world settings, we achieve 90.9% TPR and 0.3% FPR when confidence threshold is 0.5, which is 5% higher FPR and 1.7% reduction in FPR. We were able to perform better even with less training data and more testing data.

Var-CNN also outperforms prior manually extracted feature attacks, demonstrating the strength of our attack.

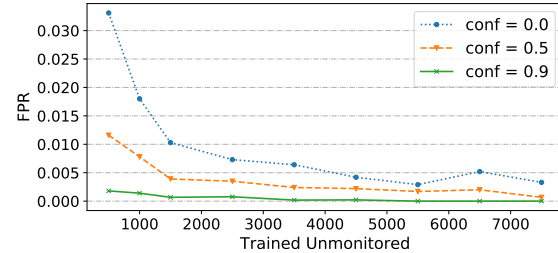


Figure 9: The Var-CNN Ensemble FPR as a function of the number of trained unmonitored sites for three different confidence settings.

With confidence threshold of 0, our Var-CNN Ensemble achieves a 93.0% TPR with a 0.7% FPR. While the TPR is higher than  $k$ -FP [14] (strongest prior attack), the higher FPR makes the attack harder to scale to larger open-world scenarios in which the client can visit more unmonitored sites. Instead, we can apply a confidence threshold of 0.5, which allows us to achieve 0.2% lower FPR compared to  $k$ -FP, while increasing the TPR by 2.9%. We show that Var-CNN can result in more successful attacks than any existing manually attacks, while remaining protocol-oblivious. We summarize all of results and comparisons in Table 2.

#### 4.2.4 Var-CNN scaling with training data

As seen in Figure 7, the training time increases linearly with the number of trained unmonitored websites in the open-world (with fixed number of trained monitored instances). In addition, it is fairly easy to parallelize CNNs with more GPUs. In comparison, Panchenko et al. [31] reported both their attack and that of Wang et al. [40] scale super-linearly with the amount of training data. Thus, Var-CNN allows an attacker to efficiently take advantage of a large training set. Moreover, recently it has been observed that in addition to being able to compute on big data, deep learning models scale better in classification performance than other machine learning techniques such as SVMs [25]. Thus, a Var-CNN-like attack is a strong candidate for an adversary with the ability to collect large amounts of training data.

#### 4.2.5 Attacks in larger open-worlds

In this section, we investigate how attacker accuracy scales with the number of trained unmonitored instances to reason about how viable our attack would be in larger open-world scenarios. In particular, we discuss how we can keep the FPR low at larger scales, since false positives are often the limiting factor at very large scales. For example, with a million traces of unmonitored websites, a FPR of even 0.1% results in 1,000 false positives.

Table 2: Closed- and open-world results of prior state-of-the-art attacks ( $k$ -NN and  $k$ -FP), prior state-of-the-art AFE attack (SDAE), and our own model (Var-CNN Ensemble), all on the Wang et al. data set [40]. Results are in %, and  $\pm$  indicates standard deviation.

Attack	Auto. Feature Extraction	Accuracy (Closed)	TPR (Open)	FPR (Open)	Precision (Open)
$k$ -NN [40]	✗	91 $\pm$ 3	85 $\pm$ 4	0.6 $\pm$ 0.4	—
$k$ -FP [14]	✗	91 $\pm$ 1	88 $\pm$ 1	0.5 $\pm$ 0.1	—
SDAE [4]	✓	88	86	2	—
Var-CNN Ensemble (conf. threshold = 0.0)	✓	93.2 $\pm$ 0.5	93.0 $\pm$ 0.5	0.7 $\pm$ 0.1	98.6
Var-CNN Ensemble (conf. threshold = 0.5)	✓	93.2 $\pm$ 0.5	90.9 $\pm$ 0.5	0.3 $\pm$ 0.1	99.3

Table 3: Comparison of Var-CNN Ensemble with a threshold of 0.5 against  $k$ -FP [14] with  $k = 3$  as the number of trained unmonitored sites changes. Results are in %.

Trained Unmonitored	TPR (Var-CNN)	TPR ( $k$ -FP)	FPR (Var-CNN)	FPR ( $k$ -FP)
0	91.60	90	50.82	75.0
1500	90.97	88	0.39	1.3
2500	91.13	88	0.35	0.7
3500	90.73	88	0.24	0.5
4500	90.93	87	0.22	0.9

First, we make an assumption that a randomly selected set of unmonitored websites is a good representation of the space of all unmonitored websites. As a result, we argue that for a network trained on a fixed set of training data, the FPR of a randomly selected testing set represents the FPR of a larger testing set. Hayes et al. [14] empirically shows this assumption, by showing that FPR stays constant when they tested on unmonitored websites while fixing the trained unmonitored websites. Furthermore, if the model learned to classify the monitored websites well, the TPR should not be significantly affected by the number of tested unmonitored pages. As shown in Table 3, FPR decreases in Var-CNN while keeping TPR constant as we increase the number of trained unmonitored websites. Combining this result with our assumption above, we believe that the attacker should perform well on potentially much larger unmonitored test set, without requiring a larger training set.

Figure 9 shows that for a minimum confidence of 0.5, the attacker achieves increasingly lower FPRs, going from 0.78% with 1000 trained unmonitored to 0.22% with 4500 and finally 0.067% with 7500. Thus, as the attacker increases the amount of training data available to Var-CNN, FPR continues to go down. In addition to FPR decreasing, Figure 8 shows that TPR does not change

much (for confidence threshold of 0 and 0.5), meaning that to achieve lower FPRs with the same TPRs, Thus, as the size of the unmonitored test set increases, the attacker could train on more unmonitored sites to get the FPR down, thereby retaining a low number of false positives without sacrificing true positives.

While it is unclear how low FPR can go for higher numbers of trained unmonitored sites, compared to prior work, we can achieve lower FPRs and higher TPRs for the same number of trained unmonitored sites. Table 3 shows a direct comparison of Var-CNN Ensemble against  $k$ -FP [14] for the exact same number of training and testing sites used for open-world. Compared to  $k$ -FP, our attack achieves higher open-world TPR at every level of trained unmonitored sites. In addition, these higher TPR levels were achieved with significantly lower FPRs. For example, with 0 trained unmonitored sites, Var-CNN Ensemble achieves a 1.6% higher TPR with a only quarter of the FPR of  $k$ -FP. For Var-CNN with a confidence threshold of 0.9, we can even achieve zero false positives after 5500 trained unmonitored, albeit at a lower TPR of around 81%. Thus, we believe that Var-CNN will scale better to larger open worlds than any prior work.

## 5 DynaFlow

As discussed earlier, prior defenses have significant drawbacks. Many do not provide formal guarantees of security which expose them to potential attacks in the future. Others often require a database of traffic patterns of websites, and thus require frequent updates to remain secure. In light of these shortcomings, we propose DynaFlow, a new website fingerprinting countermeasure based on fixed burst patterns with dynamically changing intervals between packets that provides clear security properties. At the same time, DynaFlow is highly parameterizable without a need for a precomputed database. We summarize the advantages of our defense in Table 1.

To measure the overheads of our defense, we will use the time overhead (TOH) and the bandwidth overhead (BWOH). TOH is defined to be the total transmission time of the defended trace over that without any defense. Similarly, BWOH is defined to be the total size of the defended trace in bytes over that of the original trace.

### 5.1 Details of DynaFlow

At a high level, our defense consists of three parts: (1) burst-pattern morphing, (2) constant traffic flow with dynamically changing intervals, and (3) padding the number of bursts. We describe the three components in this section.

#### 5.1.1 Burst-pattern morphing

We first note that every traffic pattern can be broken into small bursts of packets consisting of consecutive  $o$  outgoing packets followed by consecutive  $i$  incoming packets [42]. In DynaFlow, we fix a particular  $o$  and  $i$ , and morph the traffic such that every burst in all traffic looks identical to each other. To achieve this, DynaFlow adds dummy packets in either direction. The parameters  $o$  and  $i$  are tunable. After sweeping the parameters, we found that  $o = 1$  and  $i = 4$  resulted in the least overhead. That is, the traffic pattern with DynaFlow will always be of this form: one outgoing packet, four incoming packets, one outgoing packet, and so on.

#### 5.1.2 Inter-packet timing

In addition to morphing the burst patterns, we also have a constant flow of traffic, similar to BuFLo [13]. More specifically, packets are queued and sent out every  $t$  seconds according to the pre-selected burst pattern (§5.1.1). If there are no packets in the queue and we are supposed to send a packet, then DynaFlow inserts a dummy packet. We initially set the inter-packet interval  $t$  to be  $t_1$ . Then, after a fixed number of bursts  $b$ , we dynamically change the interval  $t$ . Our defense estimates the new value of  $t$  by computing a weighted sum of the average inter-packet

Table 4: Parameters of DynaFlow.

Parameter	Description
$o$	Number of outgoing packets in a burst
$i$	Number of incoming packets in a burst
$t$	Inter-packet timing
$b$	Number of bursts between adjusting $t$
$a$	Number of allowed inter-packet timing adjustments
$m$	Base burst padding

time interval of the last 20 bursts and the number of packets in the queue. Intuitively, this tracks whether we are using too many dummy packets, or conversely, setting the interval too low.

For every website, we allow up to  $a$  adjustments, and during each adjustment, the client chooses  $t$  from a limited set of available intervals  $T = \{t_1, \dots, t_k\}$ , where  $k$  is another tunable parameter. For high levels of security, we can set  $k = 1$  (or equivalently  $b = \infty$ ), which would make all traces identical except for the total number of bursts.

#### 5.1.3 The number of bursts

Combining the mechanisms from §5.1.1 and §5.1.2, the only observable difference across traces of different websites is the total number of bursts, i.e., the sizes of the traces. To hide this, we pad the number of bursts to  $\{\lfloor m \rfloor, \lfloor m^2 \rfloor, \lfloor m^3 \rfloor, \dots\}$  for some fixed  $m > 1$  by inserting dummy bursts. By padding to a power of  $m$ , we mitigate the privacy loss by limiting the number of possible traces, without incurring a huge overhead; for example, when  $m = 2$ , the bandwidth overhead is at most 100%.

Table 4 summarizes the parameters.

#### 5.1.4 Combining packets

In DynaFlow, we also introduce a small optimization on the user side to offset some of the overhead. Our defense oftentimes results in multiple outgoing requests waiting in the queue. In the case where there are two consecutive outgoing packets (before burst morphing) and the two packets total less than a single Tor packet (512 bytes), we combine them into a single packet. Small responses are also combined by the exit node. By decreasing the number of packets, packet combination mitigates the effect of delays.

## 6 DynaFlow evaluation

We now evaluate our defense, and compare DynaFlow to Tamaraw [7].

Table 5: Closed-world results against different attacks, along with time and bandwidth overheads (TOH and BWOH). Baseline indicates the case with no defense. All values are in %.

Config.	Parameters	<i>k</i> -NN [40]	<i>k</i> -FP [14]	Var-CNN	TOH	BWOH
Baseline	N/A	88.0	94.3	95.2	0	0
1	$o = 1, i = 4, t_i = 0.012, b = 160, a = 6$	17.5	45.0	46.8	31	53
	$m = 1.2, T = \{0.0012, 0.005\}$					
2	$o = 1, i = 4, t_i = 0.012, b = 80, a = 1$	6.0	18.4	18.4	38	84
	$m = 1.2, T = \{0.0015\}$					

## 6.1 Implementation

Similar to prior defenses [40, 42, 13, 7, 29], we simulate our defense by first collecting traces, and replaying the trace through our defense to generate a new trace.

## 6.2 Defense data set

To evaluate our defense, we use a data set that we collected, which consists of 100 monitored pages (90 traces each) and 9000 unmonitored pages (1 trace each). The 100 monitored pages were retrieved from Alexa’s list of the 100 most popular websites [2] while the next 9000 most popular pages make up the unmonitored class. We collected a new data set because prior released data sets do not contain enough information to simulate our defense (such as the size of unpadded packets for combining packets). We collected our traces by configuring Firefox 57.0.1 to access websites through Tor 0.2.9.9. The process was automated using Selenium 3.4.3. Each time we collected a trace, we changed the Tor circuit, to emulate the fact that different users and the adversary will access a single website using different circuits.

## 6.3 Evaluation against existing attacks

In this section, we first run DynaFlow on the data set, and then run different state-of-the-art website fingerprinting attacks on the defended data set in closed-world and open-world scenarios. We then compare against prior work, and demonstrate that DynaFlow can achieve the same level of security with lower overheads.

### 6.3.1 Closed-world defense evaluation

Table 5 illustrates the effectiveness of our defense against different attacks, including *k*-NN [40], *k*-FP [14], and Var-CNN with confidence threshold of 0.6. We tested two different configurations of DynaFlow.

DynaFlow causes substantial decreases in the accuracy of every classifier. When no defense is applied, all three attacks achieve accuracy of over 88%. We compare this to configuration 1 of our defense, which decreases

the accuracy of Var-CNN to 46.8%, *k*-FP [14] to 45.0%, and *k*-NN [40] to 17.5%. At the same time, configuration 1 has fairly low time and bandwidth overheads at 31% and 53%, respectively. Configuration 2 can lower the accuracy even further (limit all attack accuracy to below 19%), at the cost of slightly higher overheads of 38% and 84%.

### 6.3.2 Open-world defense evaluation

DynaFlow is just as effective in the realistic open-world, using the same configurations as the closed-world. With configuration 1, we reduce the TPR of all attacks to below 16%, with time and bandwidth overheads of 23% and 59%, respectively. Configuration 2 provides stronger security. For *k*-NN and *k*-FP, the FPR to TPR ratio is overwhelmingly high (69.0% to 5.9% for *k*-NN and 40.1% to 4.4% for *k*-FP). For Var-CNN, although FPR is only 0.9%, TPR is also significantly reduced to 0.6%, meaning most websites are being categorized as unmonitored websites.

## 6.4 Comparison with Tamaraw

### 6.4.1 Optimal attacker strategy

Before we compare our system with Tamaraw, we first describe the strategy of the optimal attacker. As mentioned before, we first note that there are only a finite number of possible traces once our defense is applied (assuming there is an upper bound on the number of bursts). Thus, the optimal attacker wishes to learn  $\Pr[w|t]$  (i.e., the probability that website  $w$  is visited when  $t$  is observed) for all  $w$  and  $t$  so that she could maximize her chances of classifying a website correctly. We assume that the attacker knows  $\Pr[w]$  (i.e., how likely a website is visited) for all websites  $w$ ; here, we simplify our presentation by representing all unmonitored websites as a single website  $u$ . The adversary can, for example, use the data on bandwidth consumed by a website as a proxy to estimate this probability distribution.

Table 6: Open-world results against different attacks, along with time and bandwidth overheads. The configurations are the same as Table 5. All values are in %.

Config.	k-NN [40]		k-FP [14]		Var-CNN		TOH	BWOH
	TPR	FPR	TPR	FPR	TPR	FPR		
Baseline	84.5	2.5	86.3	1.6	89.1	0.7	0	0
1	15.4	20.6	5.0	1.6	10.8	3.0	23	59
2	5.9	69.0	4.4	40.1	0.6	0.9	28	112

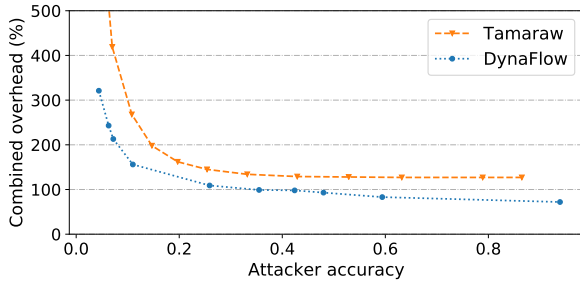


Figure 10: Sum of TOH and BWOH against optimal attacker accuracy for DynaFlow and Tamaraw.

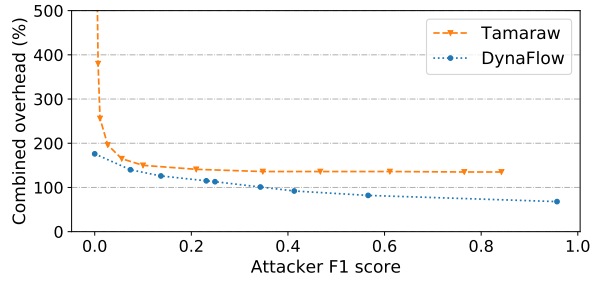


Figure 11: Sum of TOH and BWOH versus the ideal attacker’s F1 score (harmonic mean of precision and recall) for DynaFlow and Tamaraw.

The attacker starts by collecting multiple traces per website. For any given  $w$  and  $t$ , the attacker’s best estimate for  $\Pr[t|w]$  (i.e., the probability that  $t$  is observed when  $w$  is visited) is the proportion of traces of  $w$  that are identical to  $t$ . The attacker can also compute  $\Pr[t]$  as follows:

$$\Pr[t] = \sum_{w'} \Pr[w', t] = \sum_{w'} \Pr[w'] \cdot \Pr[t|w'].$$

Finally, the attacker can use Bayes’ theorem to estimate  $\Pr[w|t]$  for any given  $w$  and  $t$ :

$$\Pr[w|t] = \frac{\Pr[w] \cdot \Pr[t|w]}{\Pr[t]} = \frac{\Pr[w] \cdot \Pr[t|w]}{\sum_w \Pr[w'] \cdot \Pr[t|w']}.$$

Now suppose that the ideal attacker observes a trace  $t$ . To maximize her chances of guessing the correct website that corresponds to  $t$ , the attacker should choose a website  $w$  such that that  $\Pr[w|t]$  is maximized.

#### 6.4.2 Defense against optimal attacker

We now compare DynaFlow to Tamaraw [7]. To ensure fair comparison, we run Tamaraw on our data set and sweep its parameters in order to determine the best parameters of Tamaraw for our data set, and use the best pa-

rameters.<sup>2</sup> We assumed that  $\Pr[u] = 0.5$  (probability that user visits an unmonitored website), and  $\Pr[w_1] = \Pr[w_2]$  for all websites  $w_1$  and  $w_2$  in the set of monitored websites, though this could be easily parameterized. For our configuration, we fixed  $o = 1$ ,  $i = 4$  and  $t_1 = 0.012s$ , while varying all other parameters. We give the exact parameters used in Appendix B.

Once we apply the two defenses to our data set, we created an optimal attacker that performs the attack described in §6.4.1, for both closed-world and open-world settings. In closed-world, we plot the sum of the time and bandwidth overhead for a given attacker accuracy in Figure 10. As shown, DynaFlow achieves lower overhead than Tamaraw for all attacker accuracy. For example, DynaFlow can reduce the attacker accuracy to below 50% while keeping the sum of the overheads to 93% overhead (34% TOH and 59% BWOH). In contrast, Tamaraw’s cumulative overhead never falls below 127% (46% TOH and 81% BWOH). Even at higher levels of security, our defense remains more efficient. When the attacker’s accuracy is 20%, our defense incurs 121% total overhead (38% TOH and 84% BWOH) while Tamaraw incurs 162% total overhead (58% TOH and 104%

<sup>2</sup>We used outgoing packet interval of  $\rho_{out} = 0.012s$  and incoming packet interval of  $\rho_{in} = 0.003s$  for Tamaraw, while varying the padding parameter  $L$ .

BWOH). At 7% ideal attacker accuracy, our defense expends 213% overhead, compared to Tamaraw’s 419%. Altogether, the flexibility of DynaFlow allows for greater efficiency than Tamaraw at all security levels.

For open-world, we plot the sum of two overheads for a given F1 score. F1 score is the harmonic mean of the precision and TPR (recall), and thus is a single metric that captures both true positives and false positives. Similar to closed-world setting, DynaFlow achieves better overhead than Tamaraw as shown in Figure 11. To achieve an F1 score of 34% (29.0% TPR and 11.4% FPR), DynaFlow incurs an overhead of 101% (29% TOH and 73% BWOH). For the same F1 score, Tamaraw needs 138% overhead (40% TOH and 98% BWOH). At higher F1 scores, this gap is even larger.

## 7 Discussion and future work

In this section, we discuss the possible limitations of our work and possible avenues for future work.

**Newer models of Var-CNN.** While Var-CNN outperformed prior attacks, there are still many directions our attack could improve. Since deep learning is a rapidly accelerating field [25], applications of new model architecture breakthroughs could lead to significantly better results. For example, we used VGG-16 [36] due to the limited resources we had (in particular, the GPU memory). More powerful algorithms, such as the DenseNet CNN [17], have been shown to perform significantly better on computer vision tasks than VGG-16, and it could potentially lead to similar improvements in website fingerprinting attacks as well. In addition, recent work on Synthetic Gradients [19] could lead to RNNs with the ability to train on much longer input (like the packet sequences used in this work); since RNNs were specifically made for temporal sequences, this model might understand long-term packet interactions better than dilated convolutions.

**DynaFlow parameters.** There is a large space of parameters available to DynaFlow, and the parameters must be tuned to the network conditions and preferences of the users. For instance, if the network’s or the users’ primary concern is the latency of the connection, then we would set the inter-packet timing to be something lower, effectively trading off bandwidth for latency. If the client tends to visit pages with large HTTP responses, the number of incoming and outgoing packets per burst may need to change. In this paper, we set the parameter by fixing all but one parameters, and doing a simple sweep of the one left. In the future, we would like to find a better way to determine the best parameters, and allow easy configuration of our defense depending on the priorities.

**DynaFlow overheads.** Overheads of DynaFlow, while lower than those of Tamaraw, might still be too high for general purpose usage: for more secure configurations, the total overhead sum can exceed 100%. We hope to further reduce the overheads in future work.

**Code and data set.** To support future work, we have made our code and data set publicly available at <https://github.com/sanjit-bhat/Var-CNN--DynaFlow>.

## 8 Conclusion

In this work, we presented a new website fingerprinting attack, Var-CNN, that uses variants of CNN to automatically extract features from the traces. We show that Var-CNN not only addresses some of the shortcomings of prior attacks with manually extracted features, but also outperforms prior-art work on the same data set, achieving higher TPR and lower FPR. With this work, we demonstrated that website fingerprinting with deep learning does not require a large data set, and is feasible for a realistic attacker. Furthermore, while Var-CNN shows a lot of promise already, we believe this is only the beginning of deep learning and other automated attacks on Tor. In addition, we propose DynaFlow, a defense based on burst pattern morphing and dynamically changing flows that can achieve lower overhead than any prior work with similar security guarantees.

## 9 Acknowledgements

This work was done as part of the MIT PRIMES program while Sanjit Bhat and David Lu were students at Acton-Boxborough Regional High School. In addition to the invaluable advice from their mentor, Albert Kwon, they would like to thank Slava Gerovitch for organizing the program and providing them with the opportunity to conduct this research. They would also like to thank Srinivas Devadas for coordinating the computer science section and lending them insightful guidance and feedback.

## References

- [1] Tor metrics portal. <https://metrics.torproject.org>.
- [2] The Top 500 Sites on the Web, 2017. Available at <https://www.alexa.com/topsites>.
- [3] M. Abadi, A. Agarwal, P. Barham, E. Brevdo, Z. Chen, C. Citro, G.S. Corrado, A. Davis, J. Dean, M. Devin, S. Ghemawat, I. Goodfellow, A. Harp, G. Irving, M. Isard, Y. Jia, R. Jozefowicz, L. Kaiser, M. Kudlur, J. Levenberg, D. Mané, R. Monga, S. Moore, D. Murray, C. Olah, M. Schuster, J. Shlens, B. Steiner, I. Sutskever, K. Talwar, P. Tucker, V. Vanhoucke, V. Vasudevan, F. Viégas, O. Vinyals, P. Warden, M. Wattenberg, M. Wicke, Y. Yu, and X. Zheng. TensorFlow: Large-scale machine learning on heterogeneous systems, 2015. Software available from tensorflow.org.

- [4] K. Abe and S. Goto. Fingerprinting Attack on Tor Anonymity using Deep Learning. *Asia-Pacific Advanced Network Research Workshop*, 42:15–20, 2016.
- [5] G.D. Bissias, M. Liberatore, D. Jensen, and B.N. Levine. Privacy vulnerabilities in encrypted http streams. *Privacy Enhancing Technologies*, pages 1–11, 2006.
- [6] X. Cai, R. Nithyanand, and R. Johnson. CS-BuFLO: A Congestion Sensitive Website Fingerprinting Defense. *Privacy in the Electronic Society*, pages 121–130, 2014.
- [7] X. Cai, R. Nithyanand, T. Wang, R. Johnson, and I. Goldberg. A Systematic Approach to Developing and Evaluating Website Fingerprinting Defenses. *ACM Conference on Computer and Communications Security*, pages 227–238, 2014.
- [8] X. Cai, X. Zhang, B. Joshi, and R. Johnson. Touching from a Distance: Website Fingerprinting Attacks and Defenses. *ACM Conference on Computer and Communications Security*, pages 605–616, 2012.
- [9] H. Cheng and R. Avnur. Traffic analysis of ssl encrypted web browsing, 1998.
- [10] G. Cherubin, J. Hayes, and M. Juarez. Website Fingerprinting Defenses at the Application Layer. *Privacy Enhancing Technologies*, 2017.
- [11] F. Chollet et al. Keras, 2015. Available at <https://github.com/fchollet/keras>.
- [12] Roger Dingledine, Nick Mathewson, and Paul Syverson. Tor: The Second-Generation Onion Router. In *USENIX Security Symposium*, pages 303–320. USENIX Association, August 2004.
- [13] K. P. Dyer, S. E. Coull, T. Ristenpart, and T. Shrimpton. Peek-a-Boo, I Still See You: Why Efficient Traffic Analysis Countermeasures Fail. *IEEE Symposium on Security and Privacy*, pages 332–346, 2012.
- [14] J. Hayes and G. Danezis.  $k$ -fingerprinting: A Robust Scalable Website Fingerprinting Technique. *25th USENIX Security Symposium*, pages 1187–1203, 2016.
- [15] D. Herrmann, R. Wendolsky, and H. Federrath. Website Fingerprinting: Attacking Popular Privacy Enhancing Technologies with the Multinomial Naïve-Bayes Classifier. *ACM Workshop on Cloud Computing Security*, pages 31–42, 2009.
- [16] A. Hintz. Fingerprinting websites using traffic analysis. *Privacy Enhancing Technologies*, pages 171–178, 2003.
- [17] G. Huang, Z. Liu, L. Maaten, and K. Weinberger. Densely connected convolutional networks. *Computer Vision and Pattern Recognition*, 2017.
- [18] S. Ioffe and C. Szegedy. Batch Normalization: Accelerating Deep Network Training by Reducing Internal Covariate Shift. *JMLR Workshop and Conference*, 37:448–456, 2015.
- [19] M. Jaderberg, W.M. Czarnecki, S. Osindero, O. Vinyals, A. Graves, D. Silver, and K. Kavukcuoglu. Decoupled neural interfaces using synthetic gradients. *arXiv*, 2017.
- [20] M. Juarez, S. Afroz, G. Acar, C. Diaz, and R. Greenstadt. A critical evaluation of website fingerprinting attacks. *ACM Conference on Computer and Communications Security*, pages 263–274, 2014.
- [21] M. Juarez, M. Imani, M. Perry, C. Diaz, and M. Wright. Toward an Efficient Website Fingerprinting Defense. *European Symposium on Research in Computer Security*, pages 27–46, 2016.
- [22] A. Karpathy. CS231n Convolutional Neural Networks for Visual Recognition, 2017. Available at <http://cs231n.github.io/neural-networks-1>.
- [23] D.P. Kingma and J. Ba. Adam: A Method for Stochastic Optimization. *International Conference on Learning Representations (ICLR)*, 2014.
- [24] A. Krizhevsky, I. Sutskever, and G.E. Hinton. Imagenet classification with deep convolutional neural networks. *Advances in Neural Information Processing Systems*, pages 1097–1105, 2012.
- [25] Y. LeCun, Y. Bengio, and G.E. Hinton. Deep Learning. *Nature*, 521:436–444, 2015.
- [26] M. Liberatore and B. Levine. Inferring the source of encrypted http connections. *Proceedings of the 13th ACM Conference on Computer and Communications Security*, pages 255–263, 2006.
- [27] L. Lu, E-C. Chang, and M.C. Chan. Website fingerprinting and identification using ordered feature sequences. *Computer Security-ESORICS*, pages 199–214, 2010.
- [28] X. Luo, P. Zhou, E. W. W. Chan, W. Lee, R. K. C. Chang, and R. Perdisci. HTTPPOS: Sealing Information Leaks with Browser-side Obfuscation of Encrypted Flows. *Network and Distributed Systems Symposium*, 2011.
- [29] R. Nithyanand, X. Cai, and R. Johnson. Glove: A Bespoke Website Fingerprinting Defense. *13th ACM Workshop on Privacy in the Electronic Society*, 2014.
- [30] A. Oord, S. Dieleman, H. Zen, K. Simonyan, O. Vinyals, A. Graves, N. Kalchbrenner, A. Senior, and K. Kavukcuoglu. Wavenet: A generative model for raw audio. *arXiv*, 2016.
- [31] A. Panchenko, F. Lanze, A. Zinnen, and M. Henze. Website Fingerprinting at Internet Scale. *Network and Distributed System Security Symposium*, 2016.
- [32] A. Panchenko, L. Niessen, A. Zinnen, and T. Engel. Website Fingerprinting in Onion Routing Based Anonymization Networks. *ACM Workshop on Privacy in the Electronic Society*, pages 103–114, 2011.
- [33] M. Perry. Experimental Defense for Website Traffic Fingerprinting, 2011. Available at <https://blog.torproject.org/blog/experimental-defense-website-traffic-fingerprinting>.
- [34] V. Rimmer, D. Preuveers, M. Juarez, T. V. Goethem, and W. Joosen. Automated Feature Extraction for Website Fingerprinting through Deep Learning. *arXiv*, 2017.
- [35] O. Russakovsky, J. Deng, H. Su, J. Krause, S. Satheesh, S. Ma, Z. Huang, A. Karpathy, A. Khosla, M. Bernstein, A.C. Berg, and L. Fei-Fei. ImageNet Large Scale Visual Recognition Challenge. *International Journal of Computer Vision (IJCV)*, 115(3):211–252, 2015.
- [36] K. Simonyan and A. Zisserman. Very Deep Convolutional Networks for Large-Scale Image Recognition. *arXiv*, 2014.
- [37] P. Sirinam, M. Imani, M. Juarez, and M. Wright. Deep fingerprinting: Undermining website fingerprinting defenses with deep learning. *arXiv*, 2018.
- [38] N. Srivastava, G.E. Hinton, A. Krizhevsky, I. Sutskever, and R. Salakhutdinov. Dropout: A Simple Way to Prevent Neural Networks from Overfitting. *Journal of Machine Learning Research*, 15(1):1929–1958, 2014.
- [39] Q. Sun, D.R. Simon, Y-M. Wang, W. Russell, V.N. Padmanabhan, and L. Qiu. Statistical identification of encrypted web browsing traffic. *Proceedings of the 2002 IEEE Symposium on Security and Privacy*, pages 19–30, 2002.
- [40] T. Wang, X. Cai, R. Johnson, and I. Goldberg. Effective Attacks and Provable Defenses for Website Fingerprinting. *23rd USENIX Security Symposium*, pages 143–157, 2014.
- [41] T. Wang and I. Goldberg. Improved Website Fingerprinting on Tor. *ACM Workshop on Privacy in the Electronic Society*, 2013.
- [42] T. Wang and I. Goldberg. Walkie-Talkie: An Efficient Defense Against Passive Website Fingerprinting Attacks. *26th USENIX Security Symposium*, pages 1375–1390, 2017.

- [43] C. Wright, S. Coull, and F. Monroe. Traffic Morphing: An Efficient Defense Against Statistical Traffic Analysis. *Network and Distributed Security Symposium*, pages 237–250, 2009.
- [44] F. Yu and V. Koltun. Multi-scale context aggregation by dilated convolutions. *International Conference on Learning Representations*, 2016.

# Appendices

## A Var-CNN model details

As mentioned in §3.2.2, the only difference between Var-CNN configurations is the lack of dilated convolutions for inter-packet time intervals. In addition, the same configuration is used in open- and closed-world scenarios apart from the final softmax output for open-world having 1 more class for the unmonitored sites. For Var-CNN time input, we normalize the timestamp sequence along with the left and right inter-packet time intervals using scaling computed on the train timestamp sequence.

The convolutional feature extractor (Figure 3) in Var-CNN consists of 5 convolutional blocks, with 2, 2, 2, 3, and 3 convolutional layers in each block. Increasing the number of layers deeper in the network aids in feature extraction, along with increasing the number of filters used in the convolutional layers in each block (e.g., the number of filters is 4, 8, 8, 16, 16). Each convolutional layer uses a kernel size of 3, the same as VGG-16 [36], and is of the format Conv-ReLU-Batch Normalization. At the end of each convolutional block is a max pooling layer followed by dropout with drop rate 0.1. Compared to the dropout rates later in the model, having a low dropout rate here retains feature extraction while still regularizing the network.

After the convolutional feature extractor, we add a fully-connected layer in the format of Fully Connected-ReLU-Batch Normalization-Dropout (this format is used for every additional fully-connected layer also, except for the final layer with softmax output). This fully-connected layer has 1024 neurons and uses a drop rate of 0.4. The high number of neurons is necessary for the high-dimensional convolutional feature extractor output. Next, this layer is concatenated with the output of a separate fully-connected layer connected with the basic cumulative features. Compared to the previous fully-connected, this layer only has 32 neurons and uses 0 dropout, as the cumulative features are of a much more low-dimensional type than the convolutional feature extractor output. After concatenation, the output then flows through another fully-connected layer with 1024 neurons and a drop rate of 0.5. Using a higher drop rate here compared to previous layers is advisable since it is later in the network and thus does not disturb feature extraction. Fi-

nally, this output is sent through another fully-connected layer with no ReLU, Batch Normalization, or dropout. Instead, this layer has a neuron count equal to the number of output classes, a softmax activation function, and creates the final output probability distribution.

Var-CNN is trained with categorical cross-entropy, a standard loss function for categorical outputs. In addition, we use a batch size of 50 and run it for 200 epochs through the training data. We selected this number of epochs as we still noticed accuracy improvements with the default learning rate of 0.001 up to 100 epochs. In addition, we needed further epochs to support the learning rate scheduling scheme described in Appendix A.1. We train using the Adam optimizer, a variant of stochastic gradient descent, to increase computational efficiency and accelerate convergence [23].

### A.1 Learning rate schedules

Learning rate refers to the amount of change carried out on the network weights with each update. A higher learning rate results in more “energy” in the model, as each update causes more significant changes to the weights. While higher learning rate can reduce the time needed for model training, it can also result in overshooting local minimums in the overall optimization problem or oscillating around a local minimum without actually being able to converge [22]. For this reason, we adopt a common strategy [17] of decreasing learning rate over the training procedure, multiplying learning rate by 0.1 at 50% and 75% of the total number of training epochs. We observe that reducing learning rate later during training results in more consistent local minimums, while also reducing the amount of accuracy variance between later epochs.

## B DynaFlow and Tamaraw parameters

Here, we present the parameters we used for DynaFlow and Tamaraw.

For all configurations of DynaFlow, we set  $t_1 = 0.012$ ,  $o = 1$ , and  $i = 4$ . For all configurations of Tamaraw [7], we set  $p_{out} = 0.012$  and  $p_{in} = 0.003$ . Table 7 shows the configurations and respective F1 Score and accuracy of the ideal attacker.

Table 7: Closed-world accuracy and F1 Score of optimal attacker for each configuration of DynaFlow and Tamaraw.

Defense	Optimal Closed-world Accuracy	Optimal F1 Score	Parameters
DynaFlow	93.9	95.7	$a = \infty, b = 20, T = \{0.0012, 0.005\}, m = 1.0002$
DynaFlow	59.4	56.6	$a = 7, b = 160, T = \{0.0012, 0.005\}, m = 1.02$
DynaFlow	48.0	41.3	$a = 7, b = 160, T = \{0.0012, 0.005\}, m = 1.1$
DynaFlow	42.4	34.3	$a = 4, b = 160, T = \{0.0012, 0.005\}, m = 1.1$
DynaFlow	35.5	24.9	$a = 4, b = 160, T = \{0.0012, 0.005\}, m = 1.2$
DynaFlow	36.2	23.1	$a = 1, b = 80, \text{ and } T = \{0.0015\}, m = 1.02$
DynaFlow	25.9	13.7	$a = 1, b = 80, \text{ and } T = \{0.0015\}, m = 1.1$
DynaFlow	18.7	7.4	$a = 1, b = 80, \text{ and } T = \{0.0015\}, m = 1.2$
DynaFlow	11.0	0.0	$a = 1, b = 80, \text{ and } T = \{0.0015\}, m = 1.5$
DynaFlow	7.2	0.0	$a = 1, b = 80, \text{ and } T = \{0.0015\}, m = 2$
DynaFlow	6.3	0.0	$a = 1, b = 80, \text{ and } T = \{0.0015\}, m = 2.3$
Tamaraw	86.5	84.2	$L = 1$
Tamaraw	78.9	76.5	$L = 2$
Tamaraw	63.2	61.1	$L = 5$
Tamaraw	52.9	46.7	$L = 10$
Tamaraw	42.9	34.8	$L = 20$
Tamaraw	33.2	21.0	$L = 50$
Tamaraw	25.4	10.0	$L = 125$
Tamaraw	19.7	5.6	$L = 250$
Tamaraw	14.7	2.7	$L = 500$
Tamaraw	10.8	1.1	$L = 1000$
Tamaraw	7.0	0.7	$L = 2000$
Tamaraw	4.7	0.4	$L = 4000$